Carbohydrate Polymers 117 (2015) 11–18

Contents lists available at ScienceDirect

Carbohydrate Polymers

journal homepage: www.elsevier.com/locate/carbpol

Graft copolymerization of ethyl acrylate onto tamarind kernel powder, and evaluation of its biodegradability

Alicia del Real[a], Daniela Wallander[b], Alfredo Maciel[b,*], Gerardo Cedillo[b], Herminia Loza[c]

[a] Departamento de Nanotecnología, Centro de Física Aplica y Tecnología Avanzada, Universidad Nacional Autónoma de México, Campus Juriquilla, Querétaro C.P. 76230, Qro., Mexico
[b] Instituto de Investigaciones en Materiales, Universidad Nacional Autónoma de México, 04510 Mexico DF, Mexico
[c] Departamento de Bioquímica, Facultad de Química, Universidad Nacional Autónoma de México, Cd. Universitaria, 04510 México DF, Mexico

ARTICLE INFO

Article history:
Received 24 June 2014
Received in revised form 27 August 2014
Accepted 8 September 2014
Available online 28 September 2014

Keywords:
Biodegradable polymer
Tamarind seed polysaccharide
Poly(ethyl acrylate)
Graft polymer

ABSTRACT

In the present study, tamarind kernel powder and ethyl acrylate were reacted by free radical polymerization to synthesize a grafted copolymer soluble in water. The grafted copolymer was analyzed by Fourier transform infrared spectroscopy (FTIR) and nuclear magnetic resonance (NMR); FTIR showed a shift of the vibration of R—CO—OR′ from 1258 cm^{-1} to 1253 cm^{-1}. This shift appeared because of the grafting copolymerization. Films were prepared to study the mechanical properties and the biodegradation of this material. The mechanical properties of the grafted copolymer were found to lie between those of the parent polymers, suitable for disposable products. The new grafted copolymer manifested a steady process of biodegradation under incubation with the bacterial strain *Alicycliphilus* sp. BQ1; this was proved by scanning electron microscopy (SEM) and near infrared spectroscopy (NIR).

1. Introduction

The greater durability of synthetic polymeric materials compared to traditional, naturally-occurring materials causes serious environmental pollution due to discarded, undegraded polymers (Okada, 2002). In spite of recycling programs, most plastics still end up in municipal landfills, creating the problem of finding suitable landfill sites (Wu, 2012; Fang et al., 2005). Considerable effort has gone into developing biodegradable polymers that degrade more rapidly in the environment when discarded (Rutot, Duquese, Ydens, Degeé, & Dubois, 2001). One technique used is graft copolymerization of synthetic monomers to natural polymers.

Copolymerization, as a modifying chemical reaction, has been used to transform the properties of natural raw materials (Princia et al., 2005; Mishra & Bajpai, 2005; Nishioka, Minami, & Kosai, 1983; Ghosh, Sen, Jha, & Pal, 2010). Indeed, graft copolymerization has become an important resource for developing advanced materials, as it can improve the functional properties of polysaccharides (Chang, Hao, & Duan, 2008; Da Silva, De Paula, & Feitosa, 2007; Geresha et al., 2004), and has generated a new industry interested in vanguard research in biopolymers to increase the use of agricultural materials and their by-products and so reduce consumption of unsustainable synthetic materials.

Many agricultural products can be used in copolymers through blending with one or more additional materials. The main components of these biopolymers are storage and structural polysaccharides. Storage polysaccharides include starch and glycogen, whereas structural polysaccharides include cellulose, chitin and glucan (these polysaccharides differ in the types of linkages between the monomers; Flieger, Kantorova, Prell, & Rezanka, 2003). Natural polymers that are currently being investigated are cellulose, chitin, and agricultural products like starch, wheat and soybean proteins, and milk, among others. Starch and cellulosic fibers are the most commonly-used polysaccharides from renewable resources (Kochumalayil, Sehaqui, Zhou, & Berglund, 2010).

Polysaccharides are unique raw materials since they are the most abundant natural polymers, inexpensive, widely available in many countries, renewable, stable, hydrophilic, and modifiable (Abo-Shosha, Ibrahim, Allam, & El-Zairy, 2008). Because starch is produced by plants it is susceptible to biodegradation (Bogaert & Coszach, 2000). Lignin is another polymer that has been explored in the search to prepare a novel polymer blended with starch (Vengal & Srikumar, 2000). However, by using materials like starch, the polymer industry might come into competition with food industries and cause problems in the future. Therefore, an alternative source of polysaccharides is required.

* Corresponding author. Tel.: +52 55 56224590; fax: +52 55 56161201.
E-mail addresses: adelreal@unam.mx (A. del Real), anywallander@gmail.com (D. Wallander), macielal@unam.mx, macielalfredo@yahoo.co.uk (A. Maciel), gcedillo@iim.unam.mx (G. Cedillo), hlozat@gmail.com (H. Loza).

http://dx.doi.org/10.1016/j.carbpol.2014.09.044
0144-8617/

The polysaccharide from the tamarind seed is an important by-product of tamarind processing, but in some countries (e.g. Mexico) it is considered waste. The tamarind seed polysaccharide is a natural polymer obtained from the endosperm of *Tamarindus indica* L. Compositional analysis of tamarind kernel powder (TKP) shows that it contains carbohydrates (61.5–72.2%) (Ishola, Agbaji, & Agbaji, 1990; Bhattacharya, Bal, & Mukherjee, 1993), protein (15–20.9%), moisture (11.4–22.7%), ether extract (3.9–8%), crude fiber (2.5–8.2%), and an ash content of 2.4–4.2%. In terms of its carbohydrate structure, hydroxyls constitute the main functional groups, and are considered reaction points that are available to improve the properties of this natural polymer. Seeds of the tamarind fruit (*T. indica*) contain a cell wall storage polysaccharide that is composed of a (1 → 4)-β-D-glucan backbone substituted with side chains of α-D-xylopyranose and—β-D-galacto-pyranosyl (1 → 2)-α-D-xylopyranose linked (1 → 6) to glucose residues (Jana, Lakshman, Sen, & Basu, 2010). Recently, a polysaccharide derived from tamarind seed was envisaged as a high performance biopolymer in various applications (Kochumalayil et al., 2010; Mishra & Malhotra, 2009; Srinivasan, Ganta, Rajamanickam, Veerabhadraiah, & Varadharajan, 2011). This material has been used in the food industry and in medical applications, such as controlled drug release (Sumathi & Ray, 2002; Avachat, Guyar, & Wang, 2013; Sun, Shy, Xu, & Cao, 2013; Jana, Sen, & Basu, 2014), and recent studies have used the tamarind seed polysaccharide as a mucoadhesive. Ghosh, Sen, Jha & Bal (2010) developed a novel biodegradable polymeric flocculant based on the polyacrylamide-grafted tamarind kernel polysaccharide, while Abo-Shosha, Ibrahim, Allam, El-Zairy, and El-Zairy (2006) reported that tamarind gum/poly acrylic acid have applications as dyestuffs and textile substrates in textile printing.

Ethyl acrylate (EA), meanwhile, is an acrylic monomer used in the manufacture of a variety of polymers and copolymers as components of many commercially-important products. EA is used not only to improve the physical properties of synthetic polymers, but also to improve the properties of polymers from natural resources, such as wood pulp cellulose fibers and other renewable materials. Goñi, Gurruchaga, Vázquez, Valero, and Guzman (1994) studied the efficiency and conversion of the graft copolymerization of ethyl acrylate/alkyl methacrylate onto amylose. Gurruchaga, Goñi, Valero, and Guzman (1992) developed biocompatible materials by grafting hydroxyl methacrylates/ethyl acrylate onto amylopectin. Also, Singha and Rana (2012) functionalized cellulosic fibers by graft copolymerization of acrylonitrile/ethyl acrylate and studied moisture absorption behavior and chemical resistance in different environments.

Despite these studies and applications involving acrylates and polysaccharides, chemical reactions or physical mixtures of EA and the TKP polysaccharide have not been developed, and their subsequent degradation has not been studied.

Thus, the aim of this work focused on the chemical modification of a polysaccharide derived from a renewable resource, TKP, by grafting it with EA to synthesize a new copolymer in order to produce biodegradable films. Biodegradability of the grafted copolymer was evaluated by subjecting the material to cultures of the bacterial strain *Alicycliphilus* sp. BQ1, a dump-site insolated bacterium.

2. Experimental

2.1. Materials

Tamarind seeds were collected from waste industry in Mexico, separated manually from the pulp, and soaked in water at 90 °C before removing the testa. Next, the seeds were sun-dried for 4 h, in which the moisture at the beginning was of 12% and at the final was controlled up to a 4% and subsequently dried in an oven (Scorpion Scientific A50980) at 35 °C for 4 h more. They were then ground and separated using a mesh sieve USA—no rigorous (mant inox) series 30, 40, 50, 60, 80 and pan, helped by a rot-tap (U.S. Standard model KH59986-60) with horizontal and vertical automatic stirrer. The separating procedure was done according to ASAE Standards (1995), where 100 g. of flour was separated during 12 min. with no-rigorous stirring. The solids passed by the mesh sieve 80 were used. The monomer of ethyl acrylate was distilled in a vacuum to remove the inhibitor. The ethyl acrylate and solvents (acetone, toluene, xylene, *n*-propanol, ethanol and methanol) used in the experiments were provided by Sigma-Aldrich.

2.2. Graft copolymerization

The copolymer was prepared via free radical polymerization, with EA as the synthetic monomer and TKP as the natural polymer in a mass concentration of 70:30 (P7:3). Synthesis was conducted in solution with azobisisobutyronitrile (AIBN) as the initiator. Before polymerization, nitrogen was bubbled through the reaction mixture to remove any dissolved oxygen.

2.3. Characterization

2.3.1. Infrared spectra

Infrared spectra were recorded with an ATR-FTIR Bruker Vector spectrometer on films of TKP, PEA and the P7:3 graft copolymer. All the films were vacuum-dried for 2 h at 2 kPa.

2.3.2. Nuclear magnetic resonance

NMR spectra was recorded in a Bruker Avance 400 spectrometer, solution (PEA) and HR-MAS (P7:3) probes (BBI 5 mm with *Z* gradient and HR-MAS 4 mm) were used; in both techniques ^{1}H proton spectra were taken. PEA was taken in $CDCl_3$ and P7:3 were swollen in D_2O. Each sample was put in a 4 mm zirconia rotor and spun at 5 kHz.

2.3.3. Scanning electron microscopy

Scanning electron microscopy (SEM) was used to analyze the surface and cryogenic fracture microstructures on the films with a JEOL KSM-6060LV microscope with secondary electrons. The samples were coated with gold using a vacuum sputter-coater.

2.3.4. Thermal analysis

Thermal analysis data were measured by thermogravimetry (TGA, TA Q5000IR Instrument) and modulated differential scanning calorimetry (MDSC, Q100). All measurements were performed under a nitrogen atmosphere. The heating rate for TGA analysis was 10 °C/min, and the temperature ranged from 25 °C to 550 °C. During analyses, a platinum crucible was used. For MDSC analysis, the heating rate was 3 °C/min, and the temperature range was −70 °C to 270 °C. For this analysis, the sample was contained in an aluminum crucible.

2.3.5. Tensile test

For tensile tests, specimens were prepared by die-cut (from the films) according to the ASTM 1708 norm. Five specimens were tested for each sample. The surface of all the samples was free of visible imperfections. Before the samples were tested for tension, they were dried in a Thermo Scientific vacuum oven at 40 °C and 20 kPa. Tensile tests were conducted using an Instron 5500R machine at a testing speed of 10 mm/min.

2.4. Biodegradation test and its characterization

Biodegradation tests were conducted to evaluate the degradation of the grafted copolymer P7:3 by immersing it in Erlenmeyer flasks containing 25 mL minimal medium (MM) [pH 7.2] at 37 °C (composition in g–L^{-1}: KH_2PO_4, 2.0; K_2HPO_4, 7.0; $MgSO_4$–H_2O, 0.1; $ZnSO_4$–$7H_2O$, 0.001; $CuSO_4$–$7H_2O$, 1×10^{-4}; $FeSO_4$–$7H_2O$, 0.01; $MnSO_4$–$6H_2O$, 0.002) with mechanical stirring. P7:3 was used as the only carbon source in MM (Oceguera et al., 2007) to grow the *Alicyliphilus* sp. BQ1. Incubations for different intervals were conducted at 37 °C and 200 rpm. The P7:3 films were analyzed by near ATR-FTIR to identify sensitive signals of the functional groups present in P7:3 affected during the biodegradation test.

3. Results and discussion

3.1. Fourier transform infrared spectroscopy (FTIR)

The FTIR spectra of TKP, PEA and the grafted copolymer P7:3 are shown in Fig. 1a.

The FTIR spectra of the grafted copolymer P7:3 showed absorption peaks in the same regions as the raw materials, PEA and TKP, with no apparent change in frequencies. However, some bands suggest physical and chemical interactions between PEA and TKP, which are discussed separately below. Fig. 1b, in the inset, shows the interactions that generate an increase in the vibration intensity of the hydroxyl group, and a decrease in the vibration intensity of the carbonyl group may be the result of hydrogen bonds formed between TKP and EA after the synthesis of P7:3. The peak at 1448 cm^{-1} corresponds to the vibration of CH_2 (scissoring) of the alkoxy group of the synthetic polymer. The vibrations at 1258 and 1156 cm^{-1} are assigned to the stretching vibration of the (R—CO—OR′) group of the saturated esters, a part of the PEA (Socrates, 2007). The vibration frequency at 1094 cm^{-1} in PEA is due to the stretching of C—O—C link of saturated esters (Wang, Dong, & Xu, 2007). After the reaction between TKP and EA (P7:3), a shift from 1258 cm^{-1} to 1253 cm^{-1} of R—CO—OR′ group is observed. This provides evidence of EA grafting onto TKP and is also found in the NMR spectra. The main characteristic peak for TKP and P7:3 is at 3200–3300 cm^{-1} due to the hydroxyl groups of TKP (Abo-Shosha, M. H., Ibrahim, N. A., Allam, E., & El-Zairy, E., 2008). This signal increased in P7:3 while the band at 1728 cm^{-1}, assigned to the stretching vibration of the ester carbonyl group (C=O) of PEA,

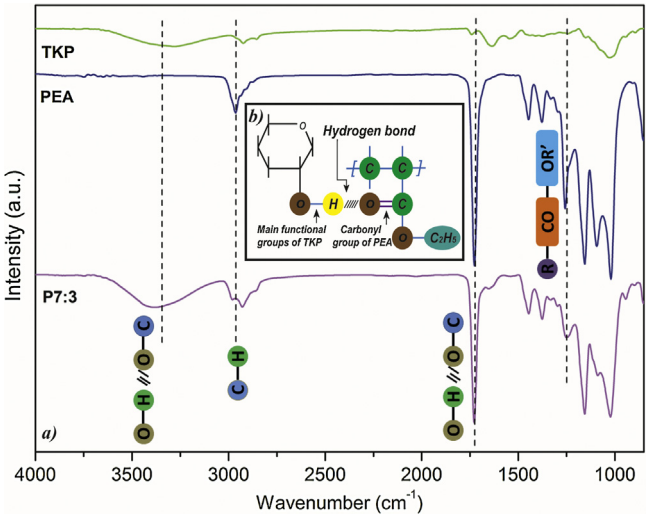

Fig. 1. (a) FTIR-ATR spectrum of TKP, PEA and sample P 7:3 and (b) physical interaction between functional groups of TKP and PEA.

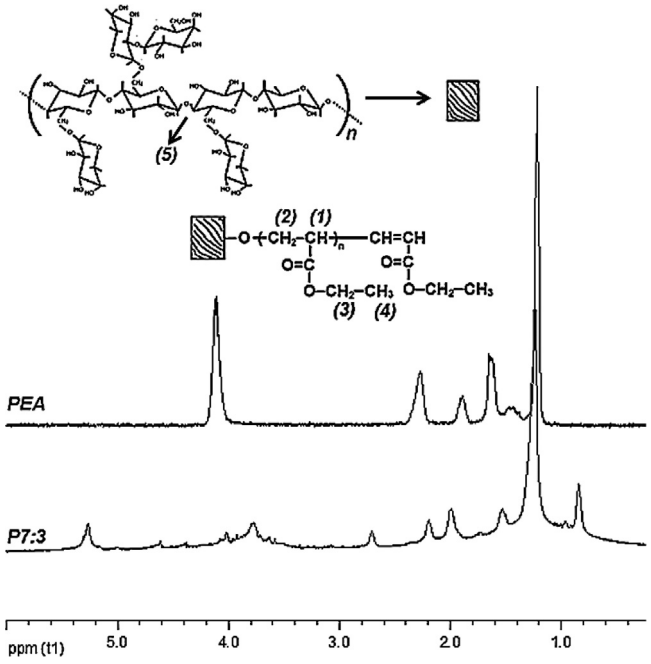

Fig. 2. ^1H NMR spectrum of PEA and P 7:3.

decreased. The interactions that generate an increase in the vibration intensity of the hydroxyl group, and a decrease in the vibration intensity of the carbonyl group, may be the result of hydrogen bonds formed between TKP and PEA after synthesis of P7:3 (Fig. 1b). The peak at 1448 cm^{-1} corresponds to the vibration of CH_2 (scissoring) of the alkoxy group of the synthetic polymer. The vibrations at 1258 and 1156 cm^{-1} are attributed to the stretching vibration of the (R—CO—OR′) group of the saturated esters, part of the PEA (Socrates, 2007). The vibration frequency at 1094 cm^{-1} in PEA is due to the stretching of the C—O—C link of saturated esters (Wang, L., Dong, W., & Xu, Y., 2007). After the reaction between TKP and EA (P7:3), a shift from 1258 cm^{-1} to 1253 cm^{-1} in the R—CO—OR′ group was seen. This provides evidence of EA grafting onto TKP, and is also found in the NMR spectra.

3.2. Nuclear magnetic resonance- proton (NMR ^1H)

^1H NMR spectrum of PEA and grafted sample P7:3 are showed in Fig. 2. PEA spectrum shows a multiplet, similar to a quartet in 4.04 ppm which correspond to (3) CH_2 and it is very close to (4) CH_3. For this reason, the spectrum present multiplet very similar to a triplet at 1.18 ppm, the integration of 3 and 4 are 2*H* and 3*H*, respectively. In the case of (1) CH and (2) CH_2, there are two signals in the main chain of the PEA (Mac Neil & Mohammed, 1995; Coehlo et al., 2008) due to tacticity. CH protons are divided in 1.85 ppm and 1.40 ppm signals; the sum of both integrations is 1*H*. There are CH_2 protons divided in 2.22 ppm and 1.6 ppm signals, the total integration of both signals is 2H. P7:3 spectrum was taken by HR-MAS. For this reason, the sample P7:3 was swollen in D_2O. To get the spectrum was necessary water suppression sequence. The signal at 5.27 ppm is due to glycosidic bonds (C—O—C) of the polysaccharide present in the TKP (5). The region from 3.0 to 4.8 ppm corresponds to the rest of polysaccharide protons. The signals corresponding to P7:3 graft copolymer are from 3.0 to 0 ppm however, the signals of (3) CH_2 and (4) CH_3 present an atypical chemical shifts. In case of (3) it is to low field (2.71 ppm) and for the shift (4) it is to high field (0.85 ppm). This behavior confirms the grafting of EA onto TKP.

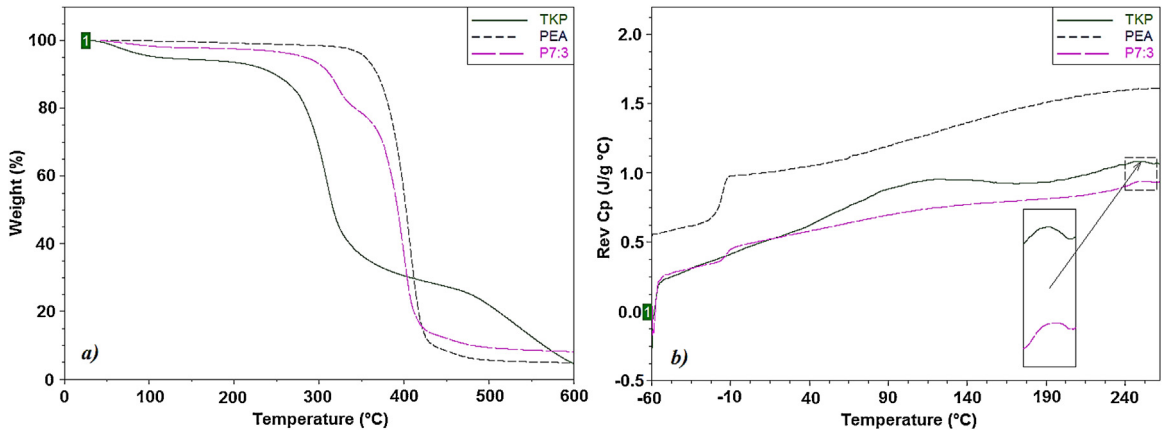

Fig. 3. (a) TGA thermograms of TKP, PEA and P7:3, (b) MDSC thermograms of TKP, PEA and P7:3.

3.3. Thermogravimetric analysis (TGA)

Thermal stability of the raw materials and the grafted copolymer was evaluated by TGA. The TKP, PEA and P7:3 thermograms are presented in Fig. 3a. The TKP thermogram showed three stages in which the sample loses weight. The first stage is due to moisture evaporation from the sample, which was 5.57% of the total mass. In the second stage, the degradation of the polysaccharide at 309 °C represents 66.17% of the total weight of the sample. The third stage (23.62%) could be attributed to the oxidative degradation of the charred residue, in the temperature range of 400–575 °C (Ouajai & Shanks, 2005). The PEA thermogram showed only one decomposition stage, which corresponded to the degradation temperature of 407 °C. This was the highest decomposition temperature range in the tested samples. The P7:3 sample showed three stages of weight loss: one of 2%, which corresponds to the water present in the sample; and a second that represented a loss of 18.73% of the initial weight of the graft copolymer. This weight loss corresponds to the amount of TKP. The degradation temperature of this stage shifts from 250 to 322 °C. This shift in the degradation temperature is due to the modification of TKP and EA that resulted from the grafting reaction. Finally, the third stage at 400 °C had a weight loss of 66.39% that could be attributed to the thermal decomposition of the PEA chains formerly grafted onto the polysaccharide. From the TGA results, it can be concluded that a graft polymer was obtained, and actually had a proportion of 80:20 of EA: TKP.

3.4. Modulated differential scanning calorimetry (MDSC)

The MDSC thermograms of TKP, PEA and P7:3 are shown in Fig. 3b. TKP presents an amorphous structure, so no melting point was detected. However, its glass transition temperature (T_g) was observed at 242 °C (Bergström, Salmen, Kochumalayil, & Berglund, 2012; Marais, Kochumalayil, Nilsson, Fogelström, & Gamstedt, 2010). The T_g of PEA was −15 °C, and no melting temperature was observed. One important characteristic of the grafted copolymer obtained is that it does not melt but, rather, degrades above 400 °C (Fig. 3a). The P7:3 sample showed two T_gs as a result of the contributions of TKP and PEA to the grafted copolymer; Cao (1999), Jones et al. (1997) mentioned that changes in the heat capacity means there were structural changes in a material. The first T_g was at −13 °C and the second at 245 °C. It is well known that the glass transition temperature increases with the length of the polymer chain, so the T_g decrease in the PEA segment of the P7:3 sample from −15 °C to −13 °C, may have been caused by the grafting reaction of PEA onto TKP.

Table 1
Mechanical properties of PEA, TKP and grafted P7:3.

	Young's modulus (MPa)	Tensile strength (MPa)	Strain (mm/mm)
TKP	2181 ± 260	22.53 ± 1.6	0.038 ± 0.004
PEA	0.69 ± 0.056	0.12 ± 0.08	1.79 ± 0.10
P7:3	549.42 ± 60	20.70 ± 1.8	0.068 ± 0.05
PS (Carvill, 2004)	3200–4200	30–60	0.04
PP (Carvill, 2004; Halimatudahliana, Ismail, & Nasir, 2002)	1100–1600	25–90	1–6

3.5. Tensile test

The tensile strength and elastic modulus of the TKP, PEA and P7:3 samples are shown in Table 1. Clearly, the elastic modulus and the strength and strain tension values of the P7:3 sample fell between those of the original polymers, TKP and PEA. Young's

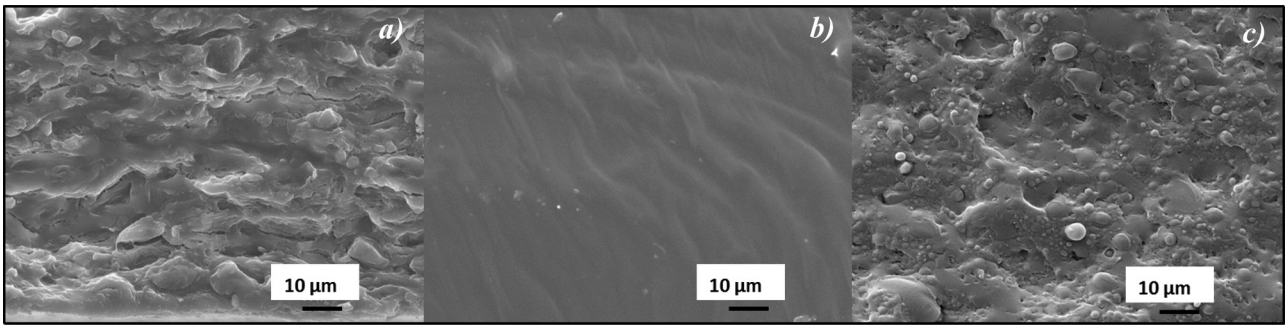

Fig. 4. Surface micrographs of frozen fractured samples (a) TKP, (b) PEA and (c) P7:3 at 1000×.

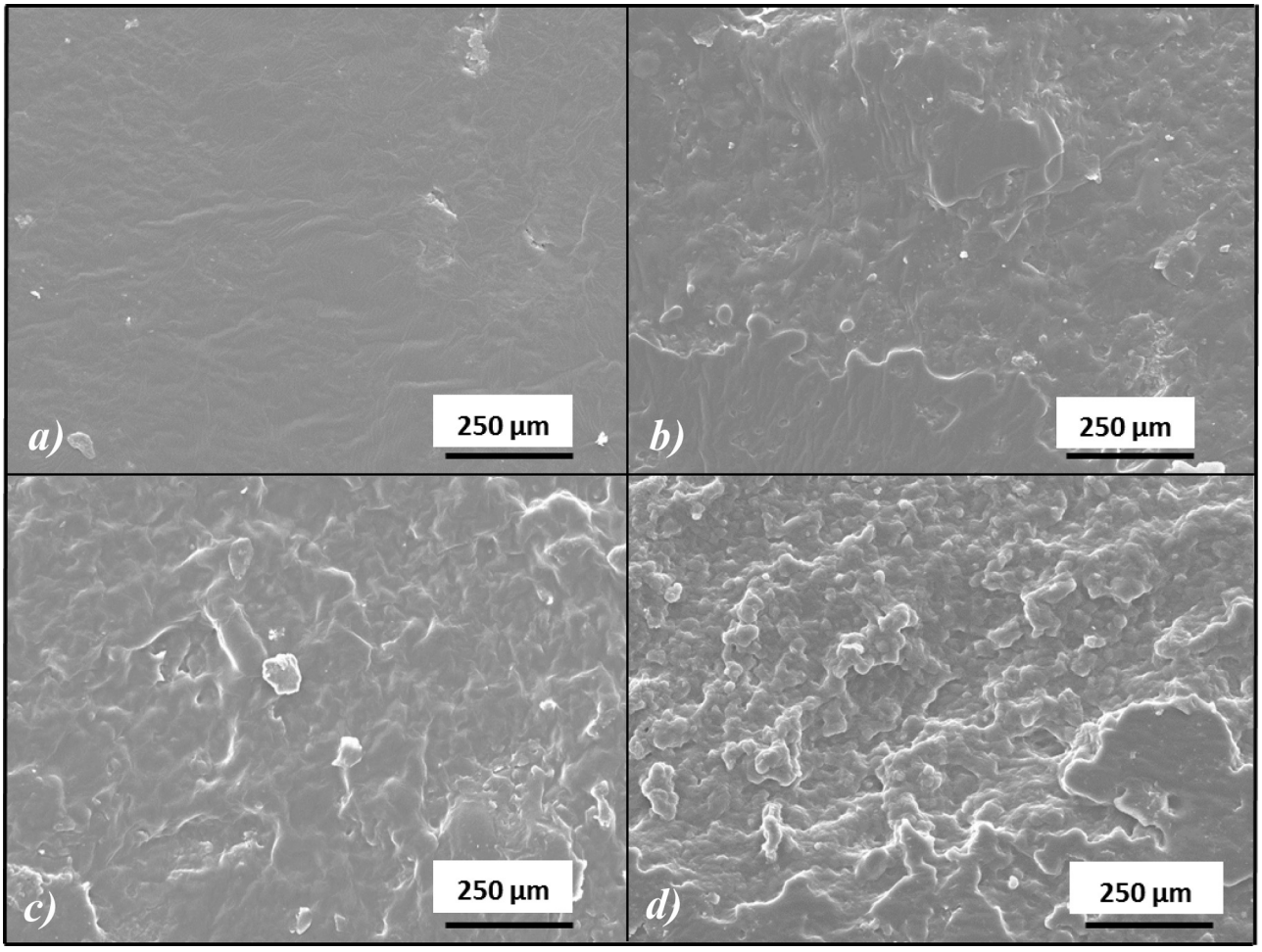

Fig. 5. Surface micrographs of P7:3 films incubated during 3 ((a) and (c)) and 6 ((b) and (d)) weeks in MM non inoculated ((a) and (b)) and inoculated ((c) and (d)) with the bacterium strain Alicyliphilus sp. BQ1. (×250).

modulus and the tensile strength of P7:3 were higher than the properties of the PEA, while the tensile strain was lower. However, P7:3 exhibited more resistance and elasticity to breakage compared to the TKP-based film. Table 1 shows a comparison of P7:3 with polystyrene and polypropylene, which are used to produce disposable materials.

Thus, adding this acrylate could be a solution to improve the mechanical properties decreasing the high stiffest present, problem found with films of this kind of polysaccharides (Aytunga & Ferhunde, 2013).

3.6. SEM

The morphology of the new surface of the frozen-fractured samples is shown in Fig. 4. The TKP samples had a rough surface with micro-domains of the disperse phase between 1 and 5 microns that may be proteins or fibers from this material (Fig. 4a). The fracture surface of PEA is smooth and presents no micro-domains, but does show an appearance of wavy fiber bundles (Fig. 4b). In the P7:3 sample there is less phase separation than in the TKP sample (Fig. 4c); however, there are micro-domains ranging from 1 to 4 microns. In addition, the surface showed a certain roughness which was intermediate between those of PEA and TKP. Micrographs support the conclusion that grafting improves compatibility between TKP and PEA.

3.7. Biodegradation test

The surfaces of the P7:3 samples incubated in MM inoculated, or not inoculated, with *Alicycliphilus* sp. BQ1, during three and six weeks, are shown in Fig. 5. The surfaces of the films incubated in MM not inoculated with BQ1 appear slightly degraded (Fig. 5a and b). However, incubation with the bacteria caused further damage to the film surface (Fig. 5c and d), indicating that P7:3 is susceptible to degradation by *Alicyliphilus* sp. BQ1, this is because the ester bonds of the copolymer present a hydrolytic or enzymatic ability to degrade (Hong et al., 2010).

The FTIR spectra of the films incubated with or without BQ1 are displayed in Fig. 6. The incubation process caused no significant changes in the spectra of these samples because of enzymatic hydrolysis as co-metabolism. However, compared to the spectrum of an unincubated sample, some changes were observed: e.g. the frequency at 3381 cm^{-1} disappeared after incubation. This signal corresponds to the stretching of the functional group OH present in the PEA and the TKP polysaccharide. The vibration at 1729 cm^{-1}, which corresponds to the carbonyl group, showed a significant increase due to the disappearance of the hydrogen bonds formed by the interaction between functional groups of TKP and PEA (Fig. 1b) through hydrolysis. The vibration frequency of the R—CO—OR′ group at 1155 cm^{-1} was affected by incubation and, as a result, showed a decrease in intensity. The vibration at 943 cm^{-1},

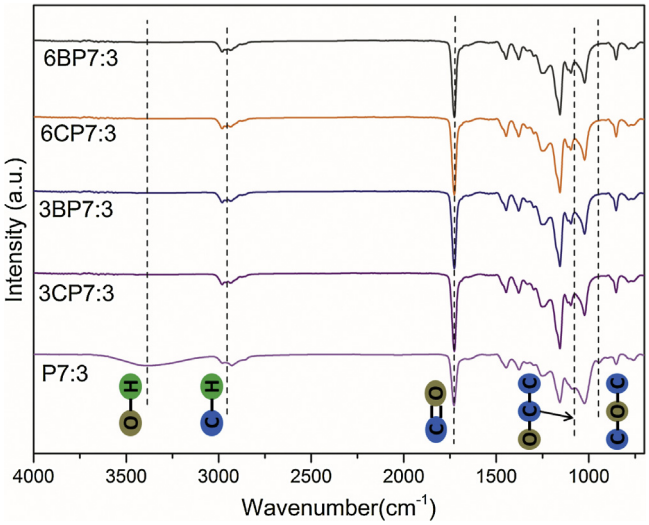

Fig. 6. FTIR spectrum of P7:3 films incubated at 3 and 6 weeks with (3BP7:3, 6BP7:3) and without (3CP7:3, 6CP7:3) *Alicycliphilus* sp. BQ1.

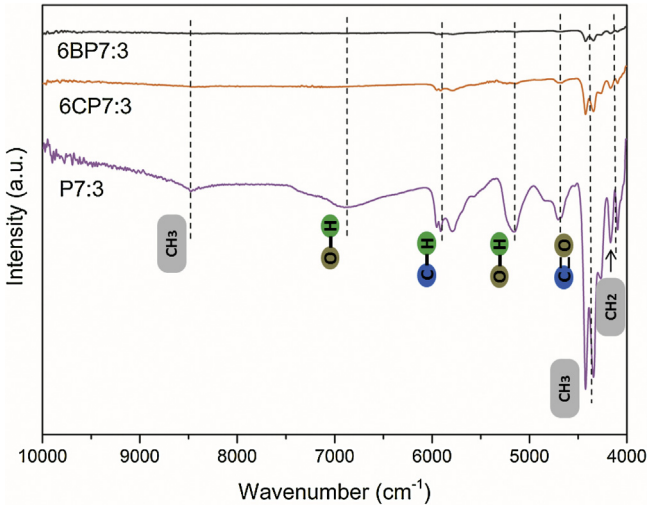

Fig. 7. NIR spectra of the sample P7:3 incubated with (6BP7:3) and without (6CP7:3) *Alicycliphilus* sp. BQ1, during 6 weeks.

which corresponds to the C—O—C group present in TKP, disappeared, representing the main point involved in the degradation process.

The NIR spectrum (Fig. 7) showed vibrations that are overtones of the C—H group at 4095, 4424 cm^{-1}, 5952–5794 cm^{-1}, and 8476 cm^{-1}. The peaks at 4095, 4169 and 4268 cm^{-1} correspond to vibrations of the CH_2 group, and the frequencies at 4424, 4324 and 8476 cm^{-1} correspond to vibrations of CH_3. The frequencies at 6900 and 5161 cm^{-1} correspond to the O—H groups. The vibrations of the O—H and CH_3 groups showed a decrease after incubation that was more marked when the films were incubated in the presence of BQ1 (6BP7:3). The signals of the CH_3, CH_2 and OH groups in the control sample (6CP7:3) decreased, probably due to water hydrolysis. However, the reduction of the signals in the sample 6BP7:3 was more severe in the presence of the bacteria, indicating that enzymatic hydrolysis by bacterial activity had a significant effect on P7:3 polymer degradation.

The DSC thermograms of the sample P7:3 without incubation and incubated with or without bacterium BQ1 are shown in Fig. 8a. The three samples had two T_g signals: the first transition occurs at −13 and −14 °C, and is due to the PEA-T_g. The T_g of the PEA did not change in any of the tested conditions. The second transition is related to the TKP-T_g. This T_g showed marked changes in the samples incubated at different temperatures in the three test conditions. The most obvious change was seen in the material incubated in the presence of BQ1 (6BP7:3) for six weeks. This supports the previously observed result which showed that even incubation in an aqueous media had an effect on the degradation of P7:3. The bacterial action through hydrolytic enzymatic activity had a more evident effect on P7:3 degradation.

Thermogravimetric analysis of the unincubated and incubated P7:3 samples, with or without the BQ1 strain, are shown in Fig. 8b. No differences in thermal properties were seen between the two samples incubated with or without BQ1. These samples inhibited a degradation stage from 280 to 390 °C. This degradation temperature is 20 °C below the degradation temperature of the unincubated P7:3 sample (260 to 370 °C). This change in the thermal properties probably occurs because of the shortening of the long chains of the PEA that were grafted onto the TKP by the degradation that occurred during incubation. The non-incubated polymer showed the three degradation stages mentioned in the discussion of Fig. 3a.

3.8. Solubility

One important characteristic of the grafted copolymer is that once prepared, it was soluble only in water. After the material was dried for the first time, it became insoluble in water and in the organic solvents toluene, xylene, *n*-propanol, ethanol and methanol. The insolubility of the copolymer after drying suggests

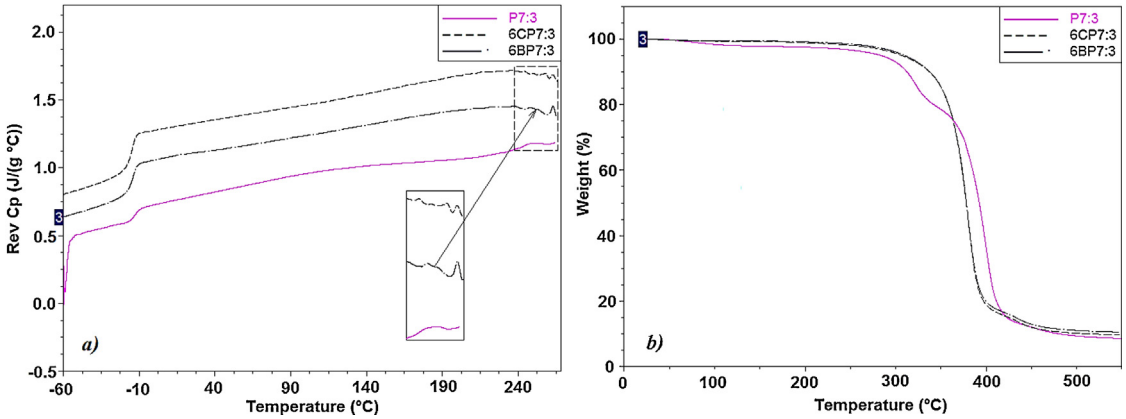

Fig. 8. (a) DSC thermogram of P7:3 not incubated and incubated during 6 weeks with (6BP7:3) or without (6CP7:3) *Alicycliphilus* sp BQ1, (b) TGA thermogram of P7:3 not incubated and incubateded during 6 weeks with (6BP7:3) and without (6CP7:3) BQ1.

that it can be synthesized under simple conditions (e.g. room temperature, water systems) to generate disposable products, thus saving energy, eliminating the need to use solvents, and reducing pollution. However, its insolubility constrains the possibility of characterizing further the graft copolymer.

4. Conclusions

Ethyl acrylate was successfully grafted onto tamarind kernel powder via free radical polymerization, as confirmed by the shift signals observed with FTIR and NMR ^{1}H. The mechanical properties of this new copolymer lie between those of the two parent polymers, though its tensile strain increased, compared to that of the pure tamarind kernel powder films. The mechanical properties of this new copolymer are adequate for disposable products. The incubation experiments revealed that P7:3 surface shows an erosion in the samples incubated and NIR displayed a reduction of signals showing that the copolymer developed can be degraded by a soil bacterium, *Alicycliphilus* sp. BQ1, suggesting that it may be biodegradable under environmental conditions. Therefore, the use of these materials would prevent environmental damage. The new copolymer is a water-based moldable material, which is important for reducing solvent use and energy consumption during processing. For these reasons, it can be considered an environmentally friendly copolymer.

Acknowledgements

This work was supported by Mexico's *Consejo Nacional de Ciencia y Tecnología* (CONACYT). The authors thank to Esteban Fregoso, Ernesto Sánchez Colín and Genoveva Hernández Padrón for their technical support, and Martín Pedro Vargas Suarez and Luz Elena Moreno for their assistance in the biodegradation test. The material developed in this research has been protected in Mexico under Patent Application Number MX/a/2013/008966.

References

Abo-Shosha, M. H., Ibrahim, N. A., Allam, E., El-Zairy, M. R., & El-Zairy, E. M. (2006). Synthesis and characterization of polyacrylic acid/dexy 85 and polyacrylic acid/gum arabic adducts. *Journal of Applied Polymer Science*, *101*, 4290–4300.

Abo-Shosha, M. H., Ibrahim, N. A., Allam, E., & El-Zairy, E. (2008). Preparation and characterization of polyacrylic acid/karaya gum and polyacrylic acid/tamarind seed gum adducts and utilization in textile printing. *Carbohydrate Polymers*, *74*, 241–249.

ASAE Standards. (1995). *5319.2. Methods for determining and expressing fineness of feed materials by sieving*. Michigan: ASAE, St. Joseph.

Avachat, A., Guyar, K. N., & Wang, K. V. (2013). Development and evaluation of tamarind seed xyloglucan-based mucoadhesive buccal films of rizatriptan benzoate. *Carbohydrate Polymers*, *91*, 537–542.

Aytunga, A. K., & Ferhunde, U. S. (2013). Thermal mechanical and water adsorption properties of corn starch–carboxymethylcellulose/methyl cellulose biodegradable films. *Journal of Food Engineering*, *114*, 123–131.

Bergström, E. M., Salmen, L., Kochumalayil, J., & Berglund, L. (2012). Plasticized xyloglucan for improved toughness—Thermal and mechanical behavior. *Carbohydrate Polymers*, *87*, 2532–2537.

Bhattacharya, S., Bal, S., & Mukherjee, R. K. (1993). Some physical and engineering properties of tamarind (*Tamarindus indica*) kernel. *Journal of Food Science and Technology*, *31*(5), 372–376.

Bogaert, J. C., & Coszach, P. (2000). Poly(lactic acid): A potential solution to plastic waste dilemma. *Macromolecular Symposia*, *153*, 287–303.

Cao, J. (1999). Mathematical studies of modulated differential scanning calorimetry I. Heat capacity measurements. *Thermochimica Acta*, *325*(2), 101–109.

Carvill, J. (2004). *Mechanical engineer's data handbook* (1st ed.). , ISBN 0750619600.

Chang, Q., Hao, X., & Duan, L. (2008). Synthesis of cross linked starch-graft polyacrylamide-*co*-sodium xanthate and its performances in wastewater treatment. *Journal of Hazardous Materials*, *159*, 548–553.

Coehlo, F. J., Carvalho, E. Y., Marques, D. S., Popov, A. V., Percec, V., Goncalves, P. M., et al. (2008). Synthesis of poly(ethyl acrylate) by single electron transfer-degenerative chain transfer living radical polymerization in water catalyzed by $Na_2S_2O_4$. *Journal of Polymer Science, A: Polymer Chemistry*, *46*, 421–432.

Da Silva, D. A., De Paula, R. C. M., & Feitosa, J. P. A. (2007). Graft copolymerization of acrylamide onto cashew gum. *European Polymer Journal*, *43*, 2620–2629.

Fang, J. M., Fowler, P. A., Escrig, C., Gonzalez, R., Costa, J. A., & Chamudis, L. (2005). Development of biodegradable laminate films derived from naturally occurring carbohydrate polymers. *Carbohydrate Polymers*, *60*, 39–42.

Flieger, M., Kantorova, M., Prell, A., & Rezanka, T. (2003). Biodegradable plastics from renewable sources. *Folia Microbiological*, *48*(1), 27–44.

Geresha, S., Gdalevskyb, G. Y., Gilboaa, I., Voorspoelsc, J., Remonc, J. P., & Kost, J. (2004). Bioadhesive grafted starch copolymers as platforms for peroral drug delivery: A study of theophylline release. *Journal of Controlled Release*, *94*, 391–398.

Ghosh, S., Sen, G., Jha, U., & Pal, S. (2010). Novel biodegradable polymeric flocculant based on polyacrylamide-grafted tamarind kernel polysaccharide. *Bioresource Technology*, *101*, 9638–9644.

Goñi, I., Gurruchaga, M., Vázquez, B., Valero, M., & Guzmán, G. M. (1994). Graft copolymerization of ethyl acrylate with alkyl methacrylates onto amylose initiated by cerium(IV). Microstructure of graft copolymers with respect to statistical copolymers. *Polymer*, *35*(7), 1535–1541.

Gurruchaga, M., Goñi, I., Valero, M., & Guzmán, G. M. (1992). Graft polymerization of hydroxylic methacrylates and ethyl acrylate onto amylopectine. *Polymer*, *33*(13), 2860–2862.

Halimatudahliana, Ismail, H., & Nasir, M. (2002). The effect of various compatibilizers on mechanical properties of polystyrene/polypropylene blend. *Polymer Testing*, *21*, 163–170.

Hong, Y., Guan, J., Fujimoto, K. L., Hashizume, R., Pelinscu, A. L., & Wagner, W. R. (2010). Tailoring the degradation kinetics of poly (ester carbonate urethane) urea thermoplastic elastomers for tissue engineering scaffolds. *Biomaterials*, *31*, 4249–4258.

Ishola, M. M., Agbaji, E. B., & Agbaji, A. S. (1990). A chemical study of *Tamarindus indica* (Tsamiya) fruits grown in Nigeria. *Journal of the Science of Food and Agriculture*, *51*, 141–143.

Jana, S., Lakshman, D., Sen, K. K., & Basu, S. K. (2010). Development and evaluation of epichlorohydrin cross-linked mucoadhesive patches of tamarind seed polysaccharide for buccal application. *International Journal of Pharmaceutical Sciences and Drug Research*, *2*(3), 193–198.

Jana, S., Sen, K. K., & Basu, S. K. (2014). In-vitro aceclofenac release from IPN matrix tablets composed of chitosan-tamarind seed polysaccharide. *Biological Macromolecules*, *65*, 241–245.

Jones, K. J., Kinshott, I., Reading, M., Lacey, A. A., Nikolopoulos, C., & Pollock, H. M. (1997). The origin and interpretation of the signals of MDSC. *Thermochimica Acta. 304-305*, 187–199.

Kochumalayil, J., Sehaqui, H., Zhou, Q., & Berglund, L. A. (2010). Tamarind seed xyloglucan—A thermostable high-performance biopolymer from non-food feedstock. *Journal of Materials Chemistry*, *20*(21), 4321–4327.

Marais, A., Kochumalayil, J. J., Nilsson, C., Fogelström, L., & Gamstedt, E. K. (2010). Toward an alternative compatibilizer for PLA/cellulose composites: Grafting of xyloglucan with PLA. *Carbohydrate Polymers*, *89*, 1038–1043.

McNeill, I., & Mohammed, H. M. (1995). A comparison of the thermal degradation behaviour of ethylene–ethyl acrylate copolymer, low density polyethylene and poly (ethyl acrylate). *Polymer Degradation and Stability*, *48*, 175–187.

Mishra, A., & Bajpai, M. (2005). Synthesis and characterization of polyacrylamide grafted copolymers of Kundoor mucilage. *Journal of Applied Polymer Science*, *98*, 1186–1191.

Mishra, A., & Malhotra, A. V. (2009). Tamarind xyloglucan: A polysaccharide with versatile application potential. *Journal of Materials Chemistry*, *19*(45), 8528–8536.

Nishioka, N., Minami, K., & Kosai, K. (1983). Homogeneous graft copolymerization of vinyl monomers onto cellulose in a dimethyl sulfoxide–paraformaldehyde solvent system III. Methyl acrylate. *Polymer Journal*, *15*, 591–596.

Oceguera, C. A., Carrillo, G. A., López, N., Bolaños, N. S., Cruz, G. M. J., Wacher, C., et al. (2007). Characterization of the polyurethanolytic activity of two *Alicycliphilus* sp. strains able to degrade polyurethane and *n*-methylpyrrolidone. *Appied and Environmental Microbiology*, *3*(19), 6214–6223.

Okada, M. (2002). Chemical synthesis of biodegradable polymers. *Progress in Polymers Sciences*, *27*, 87–133.

Ouajai, S., & Shanks, R. A. (2005). Composition, structure and thermal degradation of hemp cellulose after chemical treatments. *Polymer Degradation and Stability*, *89*, 327–335.

Princia, E., Vicinia, S., Pedemontea, E., Mulasa, A., Franceschia, E., Lucianoa, G., et al. (2005). Thermal analysis and characterization of cellulose grafted with acrylic monomers. *Thermochimica Acta*, *425*, 173–179.

Rutot, D., Duquesne, E., Ydens, I., Degée, P., & Dubois, P. (2001). Aliphatic polyester-based biodegradable materials: New amphiphilic graft copolymers. *Polymer Degradation and Stability*, *73*, 561–566.

Singha, S., & Rana, R. K. (2012). Functionalization of cellulosic fibers by graft copolymerization of acrylonitrile and ethyl acrylate from their binary mixtures. *Carbohydrate Polymers*, *87*(1), 500–511.

Socrates, G. (2007). *Infrared and Raman characteristic group frequencies tables and charts* (3rd ed.). , 139780470093078.(P/B).

Srinivasan, B., Ganta, A., Rajamanickam, D., Veerabhadraiah, B. B., & Varadharajan, M. (2011). Evaluation of tamarind seed polysaccharide as a drug release retardant. *International Journal of Pharmaceutical Science Review Research*, *9*(2), 27–31.

Sumathi, S., & Ray, A. R. (2002). Release behaviour of drugs from tamarind seed polysaccharide tablets. *Journal Pharmaceutic Science*, *5*(1), 12–18.

Sun, X., Shi, J., Xu, X., & Cao, S. (2013). Chitosan coated alginate/poly (*N*-isopropylacrylamide) beads for dual responsive drug delivery. *International Journal of Biological Macromolecules*, *59*, 273–281.

Vengal, J. C., & Srikumar, M. (2000). Processing and study of novel lignin-starch and lignin-gelatin biodegradable polymeric films. *Trends in Biomaterials and Artificial Organs*, *18*(2), 237–241.

Wang, L., Dong, W., & Xu, Y. (2007). Synthesis and characterization of hydroxypropyl methylcellulose and ethyl acrylate graft copolymers. *Carbohydrate Polymers*, *68*, 626–637.

Wu, C.-S. (2012). Characterization and biodegradation of polyester bioplastic-based green renewable composites from agricultural residues. *Polymer Degradation and Stability*, *97*, 64–71.